

# Randall-Sundrum Reality at the LHC

Vernon Barger<sup>a</sup> and Muneyuki Ishida<sup>b</sup>

<sup>a</sup>*Department of Physics, University of Wisconsin, Madison, WI 53706, USA*

<sup>b</sup>*Department of Physics, Meisei University, Hino, Tokyo 191-8506, Japan*

---

## Abstract

The radion is expected to be the first signal of the Randall-Sundrum (RS) model. We explore the possibility of finding it in the ongoing Higgs searches at the LHC. The little RS model (LRS), which has a fundamental scale at  $\sim 10^3$  TeV, is excluded over wide ranges of the radion mass from the latest  $WW$  and  $\gamma\gamma$  data by ATLAS and CMS.

*Key words:* radion, RS model, LHC

*PACS:* 04.50.-h, 11.10.Kk

---

## 1 Introduction

The Standard Model (SM) successfully explains almost all present experimental data; however, it is an unsatisfactory model to be the ultimate theory of particle physics. One of its defects is a large hierarchy between the two fundamental scales, the Planck scale  $\bar{M}_{Pl} = M_{Pl}/\sqrt{8\pi} \simeq 2 \times 10^{18}$  GeV and the weak scale  $\sim 100$  GeV, which requires an unnatural fine-tuning of model-parameters when the model is applied to weak-scale phenomenology. The Randall-Sundrum model[1] was originally proposed to solve this hierarchy problem. RS introduced the five-dimensional anti-de Sitter spacetime,

$$ds^2 = e^{-2ky} \eta_{\mu\nu} dx^\mu dx^\nu - dy^2, \quad (1)$$

with a  $S^1/Z_2$  compactified 5-th dimension, denoted as  $y \in [0, L]$ ; there are two three-branes at  $y = 0$  and  $y = L$ , called UV and IR branes, respectively. All the SM fields are confined to the IR brane in the original setup of Randall-Sundrum model, denoted as the RS1 model, and the 5-dimensional fundamental scale  $M_5$  at UV brane is scaled down to  $M_5 e^{-kL}$  at the IR brane by the warp factor  $e^{-kL}$  appearing in the metric of Eq. (1). By taking  $kL \simeq 35$ ,

the fundamental scale  $M_5 = \bar{M}_{Pl}$  is scaled down to the TeV scale. In order to suppress unwanted higher dimensional operators, which are not sufficiently suppressed by the TeV-scale cutoff on the IR brane in the RS1 model, SM gauge fields[2,3,4,5] and fermions[6,7] are considered to propagate in the bulk space. In this new setup[2,3,4,5,6,7,8,9,10,11,12,13,14,15,16], denoted as the RS model, RS can address both the hierarchy problem and fermion mass hierarchies. From the electroweak precision measurements and various flavor physics, the new Kaluza-Klein (KK) modes of the bulk SM fields are constrained to be heavier than a few TeV[2,3,4,5,6,7,8,9,10,11,12,13,14,15,16,17,18,19,20,21,22,23].

The radion  $\phi$  was introduced as a quantum fluctuation of the modulus  $L$  of the 5-th dimension. It is necessary to stabilize  $L$  to the above value. Goldberger and Wise showed that a bulk scalar field propagating in the background geometry, Eq. (1), can generate a potential that can stabilize  $L$ . [24] In order to reproduce the value  $kL \simeq 35$ , the radion should have a lighter mass than that of the Kaluza-Klein modes of all bulk fields[25]. Thus, the detection of the radion may well be expected as the first signal to indicate that the RS model is truly realized in nature.

From a purely phenomenological perspective, the fundamental scale  $M_5$  is scaled down far below the 4-dimensional  $M_{Pl}$ , by increasing the size  $kL$  of the 5-th dimension. This is known as little Randall-Sundrum (LRS) model[26]. The hierarchy problem is yet unsolved in this model. The neutral kaon mixing parameter  $\epsilon_K$  gives a strong constraint[27] on  $M_5$ , namely  $M_5 >$  several thousand TeV, in the LRS model, and this corresponds to  $kL \gtrsim 7$ . The present precision measurements of SM flavors are consistent with  $kL = 7$ . The diphoton signal at the LHC is predicted to be largely enhanced[28] in comparison to the RS model with  $kL = 35$ .

In this Letter we evaluate the production and decays of the radion. Similar analyses were done in ref.[5,28,29,30,31,32,33,34]. We refine the calculations appropriate to the LHC experiments at 7 TeV (LHC7), and consider the possibility of finding  $\phi$  in the ongoing LHC Higgs searches. We demonstrate that  $\phi$  could be found in the SM Higgs search in the  $\gamma\gamma$  and  $W^*W$  channels at LHC7, and consider the possibility of RS and LRS models being thereby tested. We find that the LRS model with  $kL = 7$  is excluded by the latest ATLAS and CMS data over a wide range of the radion mass.

## 2 Coupling to the SM particles

We define the fluctuation  $F$  of the metric and the canonically normalized radion field  $\phi$  as

$$\begin{aligned}
ds^2 &= e^{-2(ky+F)} \eta_{\mu\nu} dx^\mu dx^\nu - (1 + 2F)^2 dy^2, \\
F &= \frac{\phi(x)}{\Lambda_\phi} e^{2k(y-L)},
\end{aligned} \tag{2}$$

where  $\Lambda_\phi$  is the VEV of the radion field  $\phi(x)$ .

The couplings of the radion to the SM particles in the original RS model are composed of two parts,

$$L = L_{trace} + L_{bulk}, \tag{3}$$

where  $L_{trace}$  is determined from general covariance[24,29,30] to be

$$\begin{aligned}
L_{trace} &= \frac{\phi}{\Lambda_\phi} T_\mu^\mu(SM). \\
T_\mu^\mu(SM) &= T_\mu^\mu(SM)^{tree} + T_\mu^\mu(SM)^{anom} \\
T_\mu^\mu(SM)^{tree} &= \sum_f m_f \bar{f} f - 2m_W^2 W_\mu^+ W^{-\mu} - m_Z^2 Z_\mu Z^\mu + 2m_h^2 h^2 - \partial_\mu h \partial^\mu h \\
T_\mu^\mu(SM)^{anom} &= -\frac{\alpha_s}{8\pi} b_{QCD} \sum_a F_{\mu\nu}^a F^{a\mu\nu} - \frac{\alpha}{8\pi} b_{EM} F_{\mu\nu} F^{\mu\nu}.
\end{aligned} \tag{4}$$

Here  $T_\mu^\mu(SM)$ , the trace of the SM energy-momentum tensor, which is defined by  $\sqrt{-g} T_{\mu\nu}(SM) = 2 \frac{\delta(\sqrt{-g} L_{SM})}{\delta g^{\mu\nu}}$ , is represented as a sum of the tree-level term  $T_\mu^\mu(SM)^{tree}$  and the trace anomaly term  $T_\mu^\mu(SM)^{anom}$  for gluons and photons.  $F_{\mu\nu}^a(F_{\mu\nu})$  are their field strengths. The  $b$  values are  $b_{QCD} = 11 - (2/3)6 + F_t$ , including the top loop, and  $b_{EM} = 19/6 - 41/6 + (8/3)F_t - F_W$ , including the top and  $W$  loops.<sup>1</sup>

The  $T_\mu^\mu(SM)^{tree}$  is proportional to particle masses. The new RS model with the SM fields propagating in the bulk has an additional radion interaction,  $L_{bulk}$ , which is inversely proportional to the size of the 5-th dimension[4,5]. There is a correction to the interactions of fermions, massless gluons and photons that have couplings to a radion at tree level.

These interactions are very similar form to the interactions of SM Higgs except for an overall proportional constant,<sup>2</sup> the inverse of the radion interaction scale  $\Lambda_\phi$ , which is the VEV of  $\phi$ . It is given by

<sup>1</sup>  $F_t = \tau_t(1 + (1 - \tau_t)f(\tau_t))$  and  $F_W = 2 + 3\tau_W + 3\tau_W(2 - \tau_W)f(\tau_W)$ .  $f(\tau) = [\text{Arcsin} \frac{1}{\sqrt{\tau}}]^2$  for  $\tau \geq 1$  and  $-\frac{1}{4}[\ln \frac{\eta_+}{\eta_-} - i\pi]^2$  for  $\tau < 1$  with  $\eta_\pm = 1 \pm \sqrt{1 - \tau}$ . Here

$\tau_i \equiv \left(\frac{2m_i}{m_\phi}\right)^2$  for  $i = t, W$ .

<sup>2</sup> The overall sign of the radion couplings is opposite to that of the Higgs couplings in the most frequently used definition of  $\phi(x)$ , Eq. (2).

$$\Lambda_\phi = e^{-kL} \sqrt{\frac{6M_5^3}{k}}. \quad (5)$$

The five dimensional fundamental scale  $M_5$  is related with  $\bar{M}_{pl}$  by

$$\bar{M}_{pl}^2 = \frac{M_5^3}{k} (1 - e^{-2kL}) \simeq \frac{M_5^3}{k}. \quad (6)$$

Thus, Eq. (5) is rewritten by

$$\Lambda_\phi = \sqrt{6} \tilde{k} \frac{\bar{M}_{pl}}{k}, \quad \tilde{k} \equiv ke^{-kL}, \quad (7)$$

where  $\tilde{k}$  sets the mass scale of  $KK$ -excitations.

We adopt the radion effective interaction Lagrangian given in Ref.[5] The radion couplings to gluons and photons are

$$L_A = -\frac{\phi}{4\Lambda_\phi} \left[ \left( \frac{1}{kL} + \frac{\alpha_s}{2\pi} b_{QCD} \right) \sum_a F_{\mu\nu}^a F^{a\ \mu\nu} + \left( \frac{1}{kL} + \frac{\alpha}{2\pi} b_{EM} \right) F_{\mu\nu} F^{\mu\nu} \right] \quad (8)$$

We note that  $L_A$  has both contributions from  $L_{bulk}$  proportional to  $(kL)^{-1}$  and  $L_{trace}$  from the trace anomaly term, while only the latter term contributes for the SM Higgs case.

The radion couplings to  $W, Z$  bosons are

$$L_V = -\frac{2\phi}{\Lambda_\phi} \left[ \left( \mu_W^2 W_\mu^+ W^{-\ \mu} + \frac{1}{4kL} W_{\mu\nu}^+ W^{-\ \mu\nu} \right) + \left( \frac{\mu_Z^2}{2} Z_\mu Z^\mu + \frac{1}{8kL} Z_{\mu\nu} Z^{\mu\nu} \right) \right] \quad (9)$$

where  $V_{\mu\nu} = \partial_\mu V_\nu - \partial_\nu V_\mu$  for  $V_\mu = W_\mu^\pm, Z_\mu$  and  $\mu_i^2$  ( $i = W, Z$ ), which include the contributions from the bulk wave functions of  $W, Z$ , are represented by using  $W(Z)$  mass  $m_{W,Z}$  as  $\mu_i^2 = m_i^2 [1 - \frac{kL}{2} (\frac{m_i}{\tilde{k}})^2]$ .<sup>3</sup>

The radion couplings to the fermions are proportional to their masses.

$$L_f = -\frac{\phi}{\Lambda_\phi} m_f [I(c_L) + I(c_R)] (\bar{f}_L f_R + \bar{f}_R f_L). \quad (10)$$

<sup>3</sup> The physical masses of  $W, Z$  bosons are identified with  $\mu_i$ , not  $m_i$  ( $i = W, Z$ ); however, we neglect small difference between  $\mu_i$  and  $m_i$ , and the  $m_i$ 's are fixed with the physical masses.

The coupling is proportional to a factor  $I(c_L) + I(c_R)$  that is dependent upon the bulk profile parameters  $c_L$  and  $c_R$ . The  $I(c_L) + I(c_R)$  are given in ref.[5] as  $1 \sim 1.19$  and  $1$  for  $b\bar{b}$  and  $t\bar{t}, \tau\tau$  channels, respectively, while the value for  $c\bar{c}$  is model-dependent. We simply take  $I(c_L) + I(c_R) = 1$  for all the relevant channels:  $b\bar{b}, t\bar{t}, \tau\tau, c\bar{c}$ .<sup>4</sup>

The coupling of the radion to the IR brane-localized Higgs scalar  $h$  is given by

$$L_h = \frac{\phi}{\Lambda_\phi} (-\partial_\mu h \partial^\mu h + 2m_h^2 h^2). \quad (11)$$

The model parameters are  $kL, \Lambda_\phi, m_\phi$  and  $m_h$ . In the following we consider two values of  $kL$ :  $kL = 7$  corresponding to the LRS model and  $kL = 35$  to the original RS model. The value  $\Lambda_\phi = 3$  TeV is used[28].  $k$  is taken as  $k < M_5$  in the original RS model[1]. Here we simply take  $k = M_5$ . From Eq. (5) this corresponds to  $\tilde{k} = \Lambda_\phi/\sqrt{6}$ . The value of  $m_h$  is taken as 130 GeV unless otherwise specified, while  $m_\phi$  is treated as a free parameter. By using the effective couplings Eqs. (8) - (11) and these values of parameters, we calculate the partial decay widths and their branching ratios in §4.

### 3 Radion Production at the LHC

The production cross section of the radion  $\phi$  at hadron colliders is expected to be mainly via  $gg$  fusion, similarly to the production of a Higgs boson  $h^0$ . These cross sections are proportional to the respective partial decay widths to  $gg$ . The production cross section of  $h^0$  has been calculated in NNLO[36], and by using this result<sup>5</sup> we can directly estimate the production cross section of  $\phi$  as

$$\sigma(pp \rightarrow \phi X) = \sigma(pp \rightarrow h^0 X) \times \frac{\Gamma(\phi \rightarrow gg)}{\Gamma(h^0 \rightarrow gg)}. \quad (12)$$

By using the  $\Gamma(\phi \rightarrow gg)$  partial width given later and  $\Gamma(h^0 \rightarrow gg)$  of the SM we can predict  $\sigma(pp \rightarrow \phi X)$  in the two cases  $kL = 7, 35$ . The result is compared with the SM Higgs production in Fig. 1.

<sup>4</sup>  $c\bar{c}$  has only a tiny  $BF$ . For  $b\bar{b}$ ,  $I(c_L)+I(c_R)$  is given as 1.66 in another example[26]. In that case  $BF(\phi \rightarrow b\bar{b})$  becomes about 2.5 times larger than our present result.

<sup>5</sup> The QCD radiative corrections to the tree level  $gg \rightarrow h^0$  and  $gg \rightarrow \phi$  should be equal in the point-like approximation of the  $gg \rightarrow h^0/\phi$  interactions, so we use the tree level result for  $\Gamma(\phi \rightarrow gg)/\Gamma(h^0 \rightarrow gg)$ .

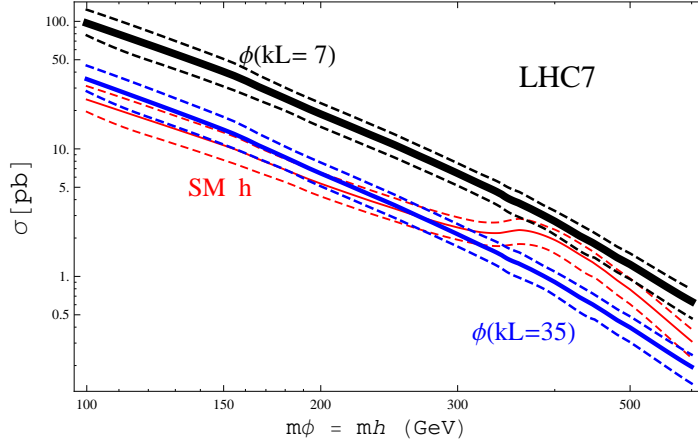


Fig. 1. The production cross sections at LHC7 of the radion  $\phi$  via  $gg$  fusion (solid blue  $kL = 35$  corresponding to the original RS model and solid thick black  $kL = 7$  to LRS model), compared with that of the SM Higgs with the same mass  $m_{h^0} = m_\phi$  (solid thin red). The  $\phi$  production cross sections are proportional to inverse-squared of  $\Lambda_\phi$ , which is taken to be  $\Lambda_\phi = 3$  TeV here. The overall theoretical uncertainties[36] are denoted by dotted lines.

The production of  $\phi$  scales with an overall factor  $(1/\Lambda_\phi)^2$ . In the  $\Lambda_\phi = 3$  TeV case, the production of  $\phi$  in the original RS model ( $kL = 35$ ) is almost the same as that of the SM Higgs boson of the same mass, while in the LRS case ( $kL=7$ ) the radion cross section exceeds that of the SM Higgs. This is because  $\phi$  production from  $gg$  fusion has an amplitude that includes a term proportional to  $1/kL$  at tree level, while there is no such term in  $h^0$  production. Our prediction of  $\sigma(\phi)$  in Fig.1 includes the  $\pm 25\%$  uncertainty associated with the theoretical uncertainty on  $\sigma(h^0)$ [36].

## 4 Radion Decay

For the radion decay channels  $\phi \rightarrow AB$ , we consider  $AB = gg, \gamma\gamma, W^+W^-, ZZ, b\bar{b}, c\bar{c}, \tau^+\tau^-, t\bar{t}$ , and  $h^0h^0$ . Their partial widths are given by the formula

$$\Gamma(\phi \rightarrow AB) = \frac{N_c}{8\pi(1 + \delta_{AB})m_\phi^2} p(m_\phi^2; m_A^2, m_B^2) \times |M|^2 \quad (13)$$

where  $p$  is the momentum of particle  $A$ (or  $B$ ) in the CM system and  $|M|^2$  represents the decay amplitude squared which are given in Table 1.<sup>6</sup>

<sup>6</sup> For the  $gg$  decay of  $\phi$  we include the radiative corrections at NNLO by using the K-factor from Higgs production. We use central values of the K-factor given in Fig. 8 of Ref.[37]: For  $m_{h^0} = 100 \sim 600$  GeV,  $K = 2.0 \sim 2.6$ . This value is about 10%

Table 1

Decay amplitudes squared  $|M|^2$  of  $\phi$  decays.  $|M|^2$  for  $ZZ$  is obtained by replacement  $W \rightarrow Z$  from  $M_{T,L}^{WW}$ .  $gg$  includes a K-factor  $K(m_\phi)$ [36].  $b_{QCD}, b_{EM}$  are given below Eq. (4) in the text.  $b\bar{b}$  includes radiative corrections[39] of running mass  $m_b(m_\phi)$  and an overall factor  $C(m_\phi)$ , but we adopt a fixed mass  $m_b = 4.5$  GeV for the kinematical factor  $(m_\phi^2/4 - m_b^2)^{3/2}$ . Similar expressions are also applied to  $t\bar{t}, c\bar{c}$  channels. The off-shell  $WW^*(ZZ^*)$  channels in the low-mass  $\phi$  case are treated in the same method as in ref.[38].

decay channel	$ M ^2$
$W^+W^-$	$2 M_T^{WW} ^2 +  M_L^{WW} ^2$
$gg$	$2 M_T^{gg} ^2 \cdot K(m_\phi)$
$\gamma\gamma$	$2 M_T^{\gamma\gamma} ^2$
$b\bar{b}$	$\frac{8}{\Lambda_\phi^2} C(m_\phi) m_b(m_\phi)^2 (\frac{m_\phi^2}{4} - m_b^2)$
$\tau^+\tau^-$	$\frac{8}{\Lambda_\phi^2} m_\tau^2 (m_\phi^2/4 - m_\tau^2)$
$h^0h^0$	$ \frac{1}{\Lambda_\phi}(m_\phi^2 + 2m_{h^0}^2) ^2$

$$M_T^{WW} = -\frac{2}{\Lambda_\phi} \left\{ \mu_W^2 - \frac{1}{2kL} \frac{m_\phi^2 - 2m_W^2}{2} \right\}$$

$$M_L^{WW} = -\left(1 - \frac{m_\phi^2}{2m_W^2}\right) M_T^{WW} - \frac{2}{\Lambda_\phi} \frac{1}{2kL} \frac{m_\phi^2(m_\phi^2/4 - m_W^2)}{m_W^2}$$

$$M_T^{gg,\gamma\gamma} = \frac{m_\phi^2}{2\Lambda_\phi kL} \left(1 + \frac{\alpha_s b_{QCD}}{2\pi} kL\right), \quad \frac{m_\phi^2}{2\Lambda_\phi kL} \left(1 + \frac{\alpha b_{EM}}{2\pi} kL\right)$$

The results of the decay branching fractions are given for the two cases  $kL = 7, 35$  in Fig. 2.

In the  $kL = 7$ (LRS model) case, there is a strong enhancement of  $BF(\phi \rightarrow \gamma\gamma)$ , in comparison to the RS model with  $kL = 35$ , as was pointed out in ref.[28]. The  $BF(\gamma\gamma)$  reaches almost  $10^{-2}$  in LRS model, while it is  $\sim 10^{-4}$  almost independent of  $m_\phi$  in RS model.  $BF(\gamma\gamma)$  is proportional to  $(1/kL)^2$  in the  $m_\phi \gtrsim 200$  GeV region in the LRS model.<sup>7</sup> This huge enhancement is from the bulk field coupling of  $\phi$  proportional to  $1/kL$ . We do not find sharp dips in  $BF(\phi \rightarrow WW, ZZ)$  around  $m_\phi \simeq 450$  GeV of Fig. 1 in ref.[28].

The total width of  $\phi$  in Fig.3 is one or two orders of magnitude smaller than that of the SM Higgs of the same mass. This is because the choice of  $\Lambda_\phi = 3$  TeV is about one order of magnitude larger than the Higgs VEV  $v = 246$  GeV. A  $\phi$  resonance would be observed with the width of the exper-

larger than the K-factor of Higgs decaying into  $gg$  in NNLO given in ref.[44] but within the uncertainty of the choice of the renormalization scale. So we assume the  $\phi$  and  $h$  K-factors are equal and adopt the value in ref.[37].

<sup>7</sup> It should be noted that in the original RS model setup where the SM fields are confined in the IR brane,  $BF(\gamma\gamma)$  steeply decreases with  $m_\phi > 200$  GeV similarly to the SM Higgs. This modified behavior comes from  $L_{bulk}$  in the new bulk field scenario of SM field.

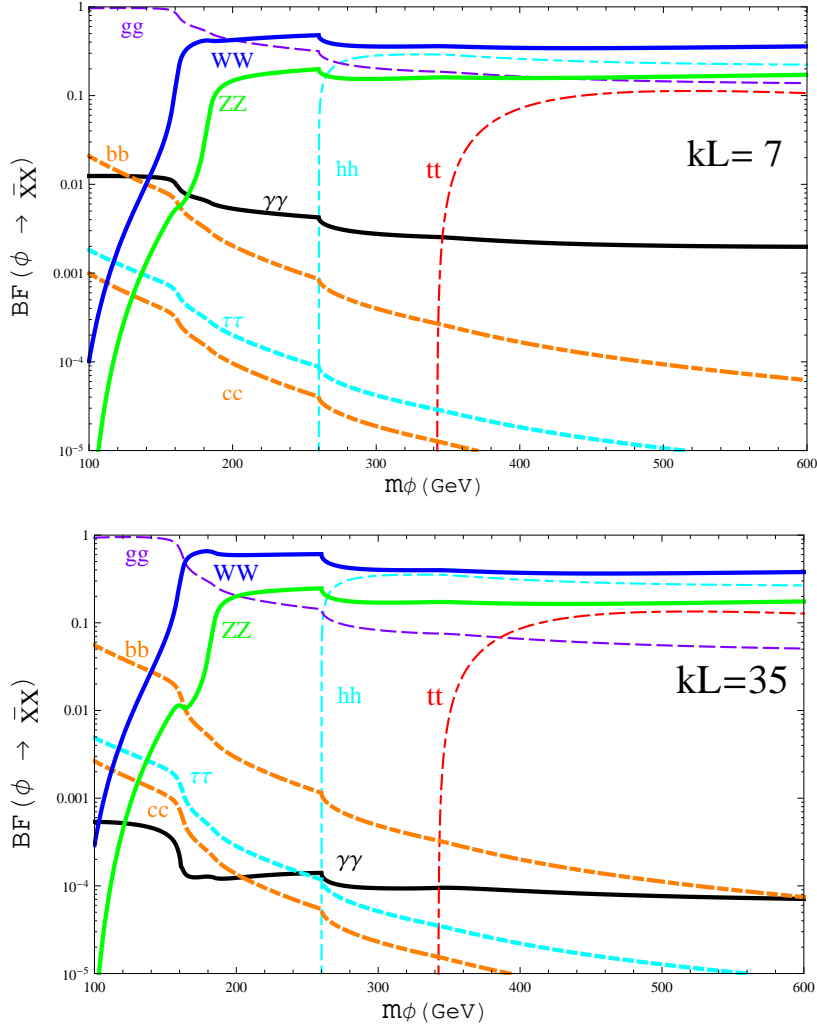


Fig. 2. Decay Branching Fractions of  $\phi$  versus  $m_\phi$ (GeV) for  $kL = 7$ (LRS model) and 35(RS model).  $m_{h^0}$  is taken to be 130 GeV.

imental resolution. The  $\Gamma(\phi \rightarrow WW)$  partial width is negligibly small compared with  $\Gamma(h^0 \rightarrow WW)$ , and thus  $\phi$  production via vector boson( $WW, ZZ$ ) fusion is unimportant at the LHC, providing another way to distinguish  $\phi$  and  $h^0$ . We note that double Higgs production via  $\phi$  decays would uniquely distinguish  $\phi$  and  $h$ .

## 5 Radion Detection compared to SM Higgs

Next we consider the detection of  $\phi$  via the  $W^+W^-$ ,  $ZZ$  and  $\gamma\gamma$  decay channels. The  $\phi$  search can be made in conjunction with the Higgs search. The properties of  $h^0$  at the LHC are well known, so we use them as benchmarks of the search for  $\phi$ .

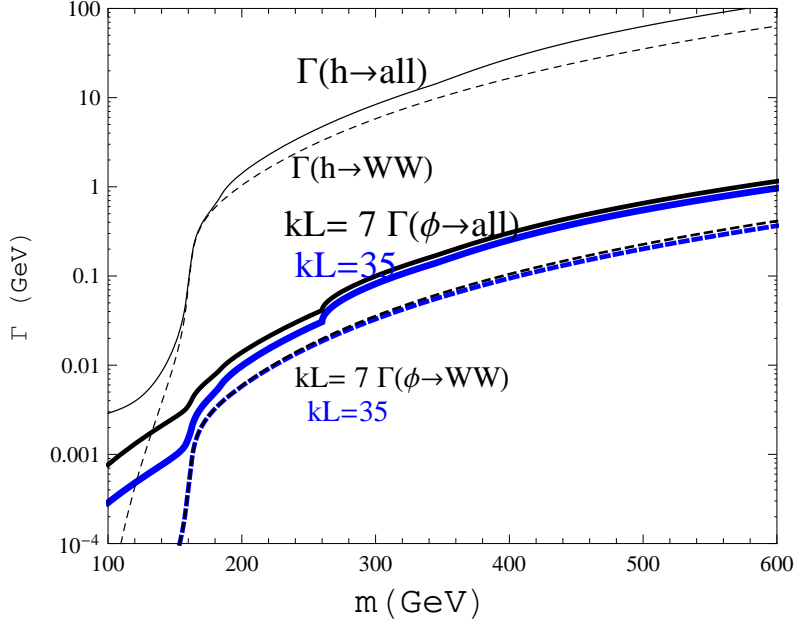


Fig. 3. Total widths (GeV) and  $W^+W^-$  partial widths of  $\phi$  compared with the SM higgs  $h^0$  with the same mass  $m = m_\phi = m_h$  (GeV). The  $\Lambda_\phi = 3$  TeV and  $kL = 7, 35$  cases are shown. For  $\Gamma(\phi \rightarrow \text{all})$  the  $m_h$  is fixed with 130 GeV. The widths of  $\phi$  are proportional to the inverse squared of  $\Lambda_\phi$ .

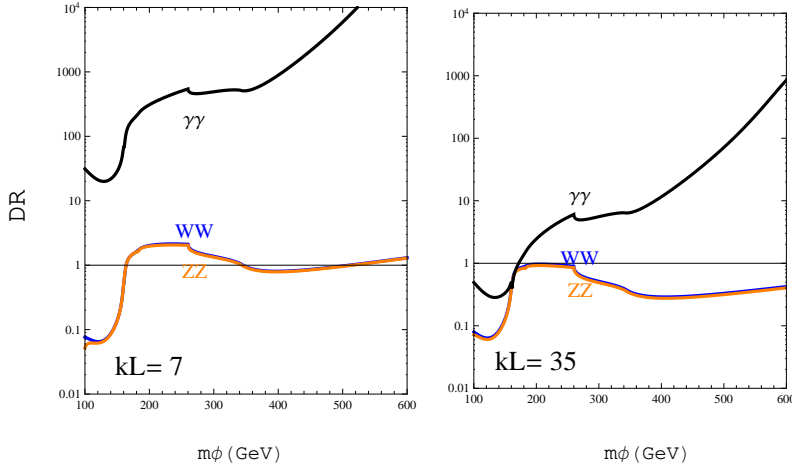


Fig. 4.  $\phi$  Detection Ratio ( $DR$ ) to the SM higgs  $h^0$  of Eq. (14) for the  $\bar{X}X = W^+W^-$  (solid blue),  $ZZ$  (dashed orange), and  $\gamma\gamma$  (solid black) final states for  $kL = 7, 35$  versus  $m_\phi$  (GeV).

The  $\phi$  detection ratio ( $DR$ ) to  $h^0$  in the  $\bar{X}X$  channel is defined[40] by

$$DR \equiv \frac{\Gamma_{\phi \rightarrow gg} \Gamma_{\phi \rightarrow \bar{X}X} / \Gamma_\phi^{\text{tot}}}{\Gamma_{h^0 \rightarrow gg} \Gamma_{h^0 \rightarrow \bar{X}X} / \Gamma_{h^0}^{\text{tot}}}, \quad (14)$$

where  $\bar{X}X = W^+W^-$ ,  $ZZ$ , and  $\gamma\gamma$ . The  $DR$  are plotted versus  $m_\phi = m_{h^0}$  in Fig. 4 for the two cases  $kL = 7$  and 35.

In mass range between the  $WW$  threshold and the  $h^0h^0$  threshold (300 GeV in the present illustration) the  $\phi$  to  $h^0$  detection ratio is relatively large in both  $WW$  and  $ZZ$  channels. The  $DR$  is almost 2 in the  $kL = 7$  case. The  $DR$  in  $\gamma\gamma$  channel increases rapidly in the large  $m_\phi = m_{h^0}$  region since  $\Gamma_{h^0 \rightarrow \gamma\gamma}$  steeply decreases with increasing  $m_h$  due to the cancellation between top and  $W$  loops. So the  $\gamma\gamma$  channel used in the search for the SH Higgs in the mass range 115-150 GeV by the LHC experiments is more sensitive for the  $\phi$  search. Surprisingly large enhancements of  $DR$  in the  $\gamma\gamma$  channel are predicted in this mass region in the  $kL = 7$  case. This is because the  $BF(\phi \rightarrow \gamma\gamma)$  is hugely enhanced in LRS model, as explained in the previous section. The  $\phi$  should be detected in  $\gamma\gamma$  in the current LHC data in the LRS scenario. This possibility is checked in Fig. 5.

The cross-section of a putative Higgs-boson signal, relative to the Standard Model cross section, as a function of the assumed Higgs boson mass, is widely used by the experimental groups to determine the allowed and excluded regions of  $m_{h^0}$ . By use of the  $DR$  in Fig. 4, we can determine the allowed region of  $m_\phi$  from the present LHC data. Figure 5 shows the 95% confidence level upper limits on Higgs-like  $\phi$  signals decaying into  $\bar{X}X$  versus  $m_\phi$  for  $\bar{X}X = WW$  (ATLAS[41], CMS[42]) and  $\gamma\gamma$  (ATLAS[43]).

For the LRS model with  $kL = 7$ ,  $m_\phi$  is excluded by ATLAS data at 95% CL over the  $m_\phi$  range,  $160 < m_\phi < 220$  GeV, while for RS model  $kL = 35$  almost no regions of  $m_\phi$  are yet excluded. Similar results are found from CMS data[42].

The  $\phi$  search is also applicable to the Tevatron data. The CDF and D0 experiments excluded a SM Higgs with mass  $158 \text{ GeV} < m_{h^0} < 175 \text{ GeV}$  from data on  $WW, ZZ$  channels. The same data exclude  $\phi$  in the  $kL = 7$  case in  $m_\phi$  range,  $163 \text{ GeV} < m_\phi < 180 \text{ GeV}$ , while for  $kL = 35$ , only  $165 \text{ GeV} < m_\phi < 171 \text{ GeV}$  is excluded.

The  $\gamma\gamma$  final state is very promising for  $\phi$  detection, because the  $\phi$  to  $h^0$  detection ratio is generally very large in all the mass range of  $m_\phi$ , as shown in Fig. 4. The  $\gamma\gamma$  data of ATLAS do not show any resonance enhancements in  $110 < m < 150$  GeV (*cf.* Fig. 5, so  $\phi$  is excluded in this mass region in the LRS model ( $kL = 7$ ) case, while no  $m_\phi$  regions are excluded in the RS model with  $kL = 35$ . The radion upper limits in the diphoton channel have similar shapes of the curve for the Higgs because the detection ratios are relatively constant in this narrow mass range  $m = 110 \sim 150$  GeV: See Fig. 4.

For  $m_\phi > 150$  GeV, the  $\gamma\gamma$  signal of  $h^0$  is too small to be detected at present, but future data in this region can determine the existence of  $\phi$ .

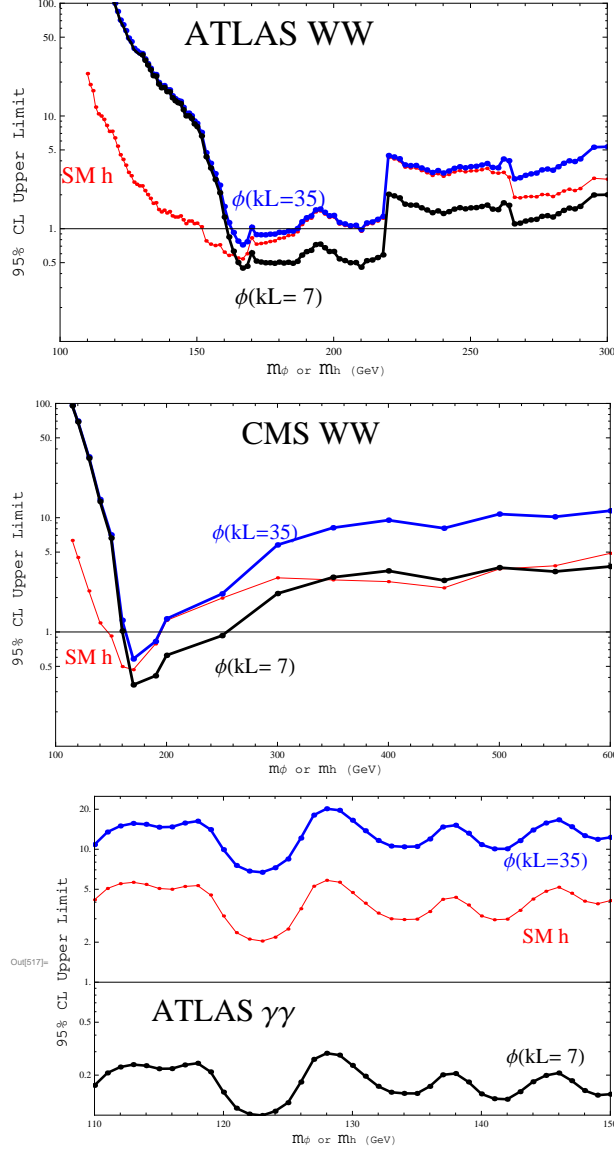


Fig. 5. The 95% confidence level upper limits on  $(1/DR) \times (\sigma_{\text{exp}}/\sigma(h^0 \rightarrow \bar{X}X))$ . This is the signal of a scalar boson decaying into  $\bar{X}X$  relative to the radion cross section [ $\sigma(\phi \rightarrow \bar{X}X) = \sigma(h^0 \rightarrow \bar{X}X) \times DR$ ] for  $\bar{X}X = WW \rightarrow l\nu l\nu$  (ATLAS[41], CMS[42]) and  $\gamma\gamma$  (ATLAS[43]) data. The cases  $kL = 35$  (solid blue) and 7 (solid black) are shown. Similar results for the SM Higgs boson are also given (red thin-solid curve).

We take  $\Lambda_\phi = 3$  TeV in our analyses. By taking larger values of  $\Lambda_\phi$ , the detection ratios of  $\phi$  decrease since the  $\phi$  production cross section is proportional to  $(1/\Lambda_\phi)^2$ . By taking  $\Lambda_\phi > 5$  TeV, all values of  $m_\phi$  become allowed by the latest ATLAS and CMS  $WW^*$  data, By taking  $\Lambda_\phi > 10$  TeV, all values of  $m_\phi$  become allowed by the latest ATLAS  $\gamma\gamma$  data,

A comment should be added here. There is a possible mixing effect[29] between the radion and SM Higgs boson through the action

$$S_\xi = -\xi \int d^4x \sqrt{-g} R H^\dagger H \quad (15)$$

where  $H$  is Higgs doublet and  $H = ((v + h^0)/\sqrt{2}, 0)$ . Because of the Higgs-like nature of the radion coupling, its effect can be very large even if the mixing angle is very small. We have excluded wide  $m_\phi$ -regions in LRS model with  $\Lambda_\phi = 3$  TeV in the no-mixing case. The effect of Eq. (15) is studied in detail in ref.[35] including a large  $\xi$  case of the RS1 model[32]. Generally speaking, when  $BF(\phi \rightarrow WW/ZZ)$  becomes larger(smaller) owing to the mixing effect,  $BF(\phi \rightarrow \gamma\gamma)$  becomes smaller(larger) than in the no-mixing case. So the  $WW/ZZ$  and  $\gamma\gamma$  channels are complementary for the detection of the radion.

## 6 Concluding Remarks

We have investigated the possibility of finding the radion  $\phi$  at the Tevatron and LHC7. The radion can be discovered in the  $WW$ ,  $ZZ$ , and  $\gamma\gamma$  channels in the search for the SM Higgs  $h^0$ . The  $WW$  signal rate can be comparable to that of the SM  $h^0$ , in the mass region  $m_\phi \sim 160$  GeV up to  $2m_{h^0}$  as shown in Fig. 4. The  $\gamma\gamma$  search channel is especially promising, since  $BF(\phi \rightarrow \gamma\gamma)$  is almost constant at  $\sim 10^{-4}$  for  $m_\phi$  below 600 GeV, and the corresponding  $\phi$  detection ratio compared to  $h^0$  is very large above  $m_\phi = 180$  GeV. Combining the  $WW, \gamma\gamma$  data of ATLAS and CMS, the LRS model with  $kL = 7$  is already excluded over wide ranges of  $m_\phi$  for  $\Lambda_\phi = 3$  TeV.

*Note added* A constraint on the mass of the first KK-graviton,  $m_{G1}$ , was reported[45] by the ATLAS collaboration from the 2-photon channel:  $m_{G1} > 0.80(1.95)$  TeV for  $k/\bar{M}_{Pl} = 0.01(0.1)$ .  $m_{G1}$  is given by  $x_1 \tilde{k}$ , where  $x_1 = 3.83$  is the first root of  $J_1$  Bessel function, and thus, a very strong constraint is obtained for the  $\Lambda_\phi$  in Eq. (7):  $\Lambda_\phi = \sqrt{6} \frac{m_{G1}}{x_1} \left(\frac{k}{\bar{M}_{Pl}}\right)^{-1}$  which gives  $\Lambda_\phi > 50(12)$  TeV for  $\frac{k}{\bar{M}_{Pl}} = 0.01(0.1)$ . However, the lower limit of  $\Lambda_\phi$  is strongly dependent upon the value of the ratio  $\frac{k}{\bar{M}_{Pl}}$ , and if this ratio is taken to be unity[46], the lower limit on  $\Lambda_\phi$  will be relaxed to a few TeV; The curvature  $k$  should be less than the Planck mass  $\bar{M}_{Pl}$  in the RS model[1].

### Acknowledgements

The authors would like to express their sincere thanks to Prof. W.-Y. Keung for his collaboration. M.I. is very grateful to the members of phenomenology institute of University of Wisconsin-Madison for hospitalities. This work was supported in part by the U.S. Department of Energy under grant No. DE-FG02-95ER40896, in part by KAKENHI(2274015, Grant-in-Aid for Young Scientists(B)) and in part by grant as Special Researcher of Meisei University.

## References

- [1] L. Randall and R. Sundrum, Phys. Rev. Lett. **83**, 3370 (1999).
- [2] H. Davoudiasl, J. L. Hewett, and T. G. Rizzo, Phys. Lett. B**473**, 43 (2000).
- [3] A. Pomarol, Phys. Lett. B **486**, 153 (2000).
- [4] T. G. Rizzo, JHEP **0206**, 056 (2002).
- [5] C. Csaki, J. Hubisz, and S. J. Lee, Phys. Rev. D**76**, 125015 (2007).
- [6] Y. Grossman and M. Neubert, Phys. Lett. B**474**, 361 (2000).
- [7] K. Agashe, A. Delgado, M. J. May, and R. Sundrum, JHEP **08**, 050 (2003).
- [8] S. Chang, J. Hisano, H. Nakano, N. Okada, and M. Yamaguchi, Phys. Rev. D**62**, 084025 (2000).
- [9] C. Csaki, J. Erlich, and J. Terning, Phys. Rev. D**66**, 064021 (2002).
- [10] J. L. Hewett, F. J. Petriello, and T. G. Rizzo, JHEP **09**, 030 (2002).
- [11] C. Csaki, C. Grojean, L. Pilo and J. Terning, Phys. Rev. Lett. **92**, 101802 (2004).
- [12] R. Contino, Y. Nomura, and A. Pomarol, Nucl. Phys. B **671**, 148 (2003).
- [13] K. Agashe, R. Contino, and A. Pomarol, Nucl. Phys. B **719**, 165 (2005).
- [14] C. Csaki, C. Grojean, J. Hubisz, Y. Shirman, and J. Terning, Phys. Rev. D**70**, 015012 (2004).
- [15] T. Gherghetta and A. Pomarol, Nucl. Phys. B **586**, 141 (2000).
- [16] S. J. Huber and Q. Shafi, Phys. Lett. B**498**, 256 (2001).
- [17] G. Burdman, Phys. Rev. D**66**, 076003 (2002); Phys. Lett. B**590**, 86 (2004).
- [18] S. J. Huber, Nucl. Phys. B **666**, 269 (2003).
- [19] K. Agashe, G. Perez, and A. Soni, Phys. Rev. D**71**, 016002 (2005).
- [20] G. Cacciapaglia, C. Csaki, J. Galloway, G. Marandella, J. Terning, and J. Weiler, JHEP **04**, 006 (2008).
- [21] C. Csaki, A. Falkowski, and A. Weiler, JHEP **09**, 008 (2008).
- [22] S. Davidson, G. Isidori, and S. Uhlig, Phys. Lett. B**663**, 73 (2008).
- [23] S. Casagrande, F. Goertz, U. Haisch, M. Neubert, and T. Pfoh, JHEP **10**, 094 (2008).
- [24] W. D. Goldberger and M. B. Wise, Phys. Rev. Lett. **83**, 4922 (1999); Phys. Lett. B**475**, 275 (2000).

- [25] C. Csaki, M. L. Graesser, and G. D. Kribs, *Phys. Rev. D* **63**, 065002 (2001).
- [26] H. Davoudiasl, G. Perez, and A. Soni, *Phys. Lett. B* **665**, 67 (2008).
- [27] M. Bauer, S. Casagrande, L. Grunder, U. Haisch, and M. Neubert, *Phys. Rev. D* **76**, 076001 (2009).
- [28] H. Davoudiasl, T. McElmurry, and A. Soni, *Phys. Rev. D* **82**, 115028 (2010).
- [29] G. F. Giudice, R. Rattazzi, and J. D. Wells, *Nucl. Phys. B* **595**, 250 (2001).
- [30] Kingman Cheung, *Phys. Rev. D* **63**, 056007 (2001).
- [31] J. L. Hewett and T. G. Rizzo, *JHEP* **08**, 028 (2003).
- [32] D. Dominici, B. Grzadkowski, J. F. Gunion, and M. Toharia, *Nucl. Phys. B* **671**, 243 (2003); *Acta Phys. Pol. B* **33**, 2507 (2002).
- [33] J. F. Gunion, M. Toharia, and J. D. Wells, *Phys. Lett. B* **585**, 295 (2004).
- [34] M. Frank, B. Korutlu, and M. Toharia, arXiv:1110.4434v1 [hep-ph].
- [35] M. Toharia, *Phys. Rev. D* **79**, 015009 (2009).
- [36] J. Baglio and A. Djouadi, arXiv:1012.0530v3 [hep-ph].
- [37] S. Catani, D. de Florian, M. Grazzini, and P. Nason, *JHEP* **07**, 028 (2003)
- [38] W.-Y. Keung and W. J. Marciano, *Phys. Rev. D* **30**, 248 (1984).
- [39] "The Higgs Hunters' Guide," J. F. Gunion, H. E. Haber, G. Kane, and S. Dawson, Perseus books 1990.
- [40] V. D. Barger and R. J. N. Phillips, "Collider Physics" Updated Edition, Westview press (1991).
- [41] The ATLAS Collaboration, preliminary result given in the presentation by M. L. Vazquez Acosta in SUSY2011 at FNAL, Aug. 30, 2011
- [42] The CMS Collaboration, "Search for the Higgs Boson Decaying to W+W in the Fully Leptonic Final State". CMS physics result, 18-Aug-2011, for the analysis CMS-HIG-11-014 on CMS public web.
- [43] The ATLAS Collaboration, CERN-PH-EP-2011-129; arXiv:1108.5895v1 .
- [44] M. Schreck and M. Steinhauser, arXiv:0708.0916v2 [hep-ph].
- [45] The ATLAS Collaboration, arXiv:1112.2194v1 [hep-ex].
- [46] H. Davoudiasl, J. L. Hewett, and T. G. Rizzo, *Phys. Rev. Lett.* **84**, 2080 (2000).